



Originally published as:

Ni, B., Cao, X., Shprits, Y., Summers, D., Gu, X., Fu, S., Lou, Y. (2018): Hot Plasma Effects on the Cyclotron-Resonant Pitch-Angle Scattering Rates of Radiation Belt Electrons Due to EMIC Waves. - *Geophysical Research Letters*, 45, 1, pp. 21—30.

DOI: <http://doi.org/10.1002/2017GL076028>



RESEARCH LETTER

10.1002/2017GL076028

Key Points:

- Both cold and hot dispersion relations are used in the calculations of EMIC wave-induced bounce-averaged pitch angle diffusion coefficients
- Hot plasma effects can significantly influence the scattering loss of radiation belt electrons induced by all the three EMIC wave bands
- The differences of diffusion coefficients are caused by the changes of resonant frequency and wave group velocity

Correspondence to:

B. Ni,
bbni@whu.edu.cn

Citation:

Ni, B., Cao, X., Shprits, Y. Y., Summers, D., Gu, X., Fu, S., & Lou, Y. (2018). Hot plasma effects on the cyclotron-resonant pitch-angle scattering rates of radiation belt electrons due to EMIC waves. *Geophysical Research Letters*, 45, 21–30. <https://doi.org/10.1002/2017GL076028>







Received 12 OCT 2017

Accepted 9 DEC 2017

Accepted article online 13 DEC 2017

Published online 4 JAN 2018

Hot Plasma Effects on the Cyclotron-Resonant Pitch-Angle Scattering Rates of Radiation Belt Electrons Due to EMIC Waves

Binbin Ni¹ , Xing Cao¹ , Yuri Y. Shprits^{2,3,4} , Danny Summers⁵ , Xudong Gu¹ , Song Fu¹ , and Yuequn Lou¹

¹Department of Space Physics, School of Electronic Information, Wuhan University, Wuhan, China, ²Helmholtz Centre Potsdam, GFZ German Research Centre for Geosciences, Potsdam, Germany, ³Institute of Physics and Astronomy, University of Potsdam, Potsdam, Germany, ⁴Department of Earth, Planetary, and Space Sciences, University of California, Los Angeles, CA, USA, ⁵Department of Mathematics and Statistics, Memorial University of Newfoundland, St. John's, Newfoundland, Canada

Abstract To investigate the hot plasma effects on the cyclotron-resonant interactions between electromagnetic ion cyclotron (EMIC) waves and radiation belt electrons in a realistic magnetospheric environment, calculations of the wave-induced bounce-averaged pitch angle diffusion coefficients are performed using both the cold and hot plasma dispersion relations. The results demonstrate that the hot plasma effects have a pronounced influence on the electron pitch angle scattering rates due to all three EMIC emission bands (H^+ , He^+ , and O^+) when the hot plasma dispersion relation deviates significantly from the cold plasma approximation. For a given wave spectrum, the modification of the dispersion relation by hot anisotropic protons can strongly increase the minimum resonant energy for electrons interacting with O^+ band EMIC waves, while the minimum resonant energies for H^+ and He^+ bands are not greatly affected. For H^+ band EMIC waves, inclusion of hot protons tends to weaken the pitch angle scattering efficiency of >5 MeV electrons. The most crucial differences introduced by the hot plasma effects occur for >3 MeV electron scattering rates by He^+ band EMIC waves. Mainly due to the changes of resonant frequency and wave group velocity when the hot protons are included, the difference in scattering rates can be up to an order of magnitude, showing a strong dependence on both electron energy and equatorial pitch angle. Our study confirms the importance of including hot plasma effects in modeling the scattering of ultra-relativistic radiation belt electrons by EMIC waves.

1. Introduction

Electromagnetic ion cyclotron (EMIC) waves are frequently observed in the Earth's magnetosphere and can be generated near the equator by the anisotropic distribution of energetic ring current protons via cyclotron instabilities (e.g., Anderson et al., 1996; Meredith et al., 2014; Min et al., 2015; Saikin et al., 2015). EMIC waves usually occur in three distinct emission bands (H^+ , He^+ , and O^+) with frequencies just below the corresponding ion gyrofrequency. Pitch-angle scattering by cyclotron-resonant interactions with EMIC waves has long been recognized to be an important loss mechanism of radiation belt electrons (Liu et al., 2012; Ni et al., 2015; Shprits et al., 2008, 2013, 2016, 2017; Summers et al., 2007a, 2007b; Summers & Thorne, 2003; Thorne & Kennel, 1971; Usanova et al., 2014) and ring current protons (Jordanova et al., 2001; Usanova et al., 2010). EMIC waves can also heat thermal electrons and heavy ions (He^+ and O^+) (Horne & Thorne, 1997; Thorne & Horne, 1997; Zhang et al., 2011) and induce efficient scattering loss of central plasma sheet protons (Cao et al., 2016; Liang et al., 2014). Further, Shprits (2009) and Cao et al. (2017) found that bounce resonance scattering by H^+ band EMIC waves can contribute to the diffusive transport of near-equatorially mirroring electrons to lower pitch angles.

The cold plasma dispersion relation (e.g., Stix, 1962) has been widely used in quantifying resonant interactions between EMIC waves and magnetospheric particles (Albert, 2003; Cao et al., 2016; Ni et al., 2015; Summers et al., 2007a, 2007b; Summers & Thorne, 2003; Xiao et al., 2011), since it readily converts the wave number to wave frequency that can be directly measured by spacecraft. However, the cold plasma approximation can seriously break down when the kinetic effects introduced by warm or hot plasmas are sufficiently strong, especially, for instance, during periods of substorm injection of hot particles from the magnetotail.

It has been found that introduction of hot ions can lead to the pronounced modification of the real part dispersion relation of EMIC waves and that the strongest deviations from the cold plasma theory occur in the regions where EMIC waves are either strongly excited or damped (e.g., Chen et al., 2013, 2011; Henning & Mace, 2014; Silin et al., 2011; Wang et al., 2016). Lee et al. (2012) showed that EMIC waves can even be excited inside the nominal stop bands of the EMIC wave spectrum in the presence of both hot protons and warm helium ions. Thus, the actual dispersive properties of EMIC waves could be poorly represented by the cold plasma dispersion relation, especially near the frequencies where the waves tend to have the strongest power spectral densities. Under such circumstances, the hot plasma dispersion relation for EMIC waves instead of the cold plasma dispersion relation needs to be implemented in calculations of quasi-linear diffusion coefficients to improve our understanding of the resonant electron scattering by EMIC waves.

This study is aimed at investigating the hot plasma effects on the EMIC wave-induced cyclotron-resonant scattering of radiation belt electrons in a realistic magnetospheric environment. By performing calculations of the quasi-linear bounce-averaged electron pitch angle diffusion coefficients using both the cold and hot plasma dispersion relations, we show that modification of the EMIC wave dispersion relation by hot protons can strongly affect the electron pitch angle scattering. We strongly suggest that the hot plasma effects should be taken into account so as to improve our understanding of the ultra-relativistic radiation belt electron dynamics, particularly during periods of geomagnetic storms and substorms.

2. Method

By assuming that the particle population can be described by bi-Maxwellian distributions (Chen et al., 2013; Gary et al., 1994; Stix, 1962), the hot plasma dispersion relation of left-hand parallel-propagating EMIC waves in a multi-ion plasma consisting of hot anisotropic protons and four cold particle species, that is, cold electrons, protons, He⁺ ions, and O⁺ ions, can be written as (e.g., Gary, 1993; Kozyra et al., 1984; Lee et al., 2017)

$$\left(\frac{ck}{\Omega}\right)^2 = 1 - \frac{\omega_{pe}^2}{\Omega} \left(\frac{1}{\Omega + |\Omega_e|} + \frac{\eta_{cp}\varepsilon_p}{\Omega - \Omega_p} + \frac{\eta_{He^+}\varepsilon_p}{4\Omega - \Omega_p} + \frac{\eta_{O^+}\varepsilon_p}{16\Omega - \Omega_p} \right) - \frac{\omega_{pe}^2\eta_{hp}\varepsilon_p}{\Omega^2} \left(A_{hp} + ((A_{hp} + 1)(\Omega - \Omega_p) + \Omega_p) \frac{Z(\zeta)}{k\alpha_{\parallel}} \right). \quad (1)$$

Here $\Omega = \omega + i\omega_i$ is the wave frequency consisting of the real part ω and imaginary part ω_i , k is the wave number, c is the speed of light, $|\Omega_e| = eB_0/m_e$ is the electron gyrofrequency, $\Omega_p = eB_0/m_p$ is the proton gyrofrequency, $\varepsilon_p = m_e/m_p$, m_e is the electron rest mass, m_p is the proton rest mass, $\omega_{pe} = (n_e e^2/m_e \varepsilon_0)^{1/2}$ is the electron plasma frequency, e is the electron charge, B_0 is the background magnetic field intensity, n_e is the electron number density, and ε_0 is the vacuum dielectric constant. We define $\eta_{cp} = n_{cp}/n_e$, $\eta_{hp} = n_{hp}/n_e$, $\eta_{He^+} = n_{He^+}/n_e$, and $\eta_{O^+} = n_{O^+}/n_e$, where n_{cp} , n_{hp} , n_{He^+} , and n_{O^+} are the number densities of the cold protons, hot protons, cold He⁺ ions, and cold O⁺ ions, respectively. Contribution to the EMIC wave dispersion relation from the hot protons is represented by the third term on the right side of equation (1); $A_{hp} = T_{\perp}/T_{\parallel} - 1$ is the temperature anisotropy of hot protons, $\alpha_{\parallel} = (2T_{\parallel}/m_p)^{1/2}$ is the parallel component of the thermal velocity, and T_{\perp} and T_{\parallel} are the perpendicular and parallel temperatures of hot protons, respectively; $\zeta = (\omega - \Omega_p)/(k\alpha_{\parallel})$ is the argument of plasma dispersion function Z (Fried & Conte, 1961). If all the particle species are assumed to be absolutely cold (i.e., the cold plasma approximation), the kinetic linear dispersion relation of parallel-propagating EMIC waves, that is, equation (1), is reduced to

$$\left(\frac{ck}{\omega}\right)^2 = 1 - \frac{\omega_{pe}^2}{\omega} \left(\frac{1}{\omega + |\Omega_e|} + \frac{\eta_p\varepsilon_p}{\omega - \Omega_p} + \frac{\eta_{He^+}\varepsilon_p}{4\omega - \Omega_p} + \frac{\eta_{O^+}\varepsilon_p}{16\omega - \Omega_p} \right), \quad (2)$$

with $\eta_p = n_p/n_e$, where $n_p = n_{cp} + n_{hp}$ is the total proton number density. Since waves undergo neither amplification nor damping in a cold plasma environment, the wave frequency ω is real.

The Doppler-shifted gyroresonance condition between parallel-propagating EMIC waves and electrons is given by the equation (Summers & Thorne, 2003),

$$\omega - kv_{\parallel} = -|\Omega_e|/\gamma, \quad (3)$$

where $\gamma = (1 - v^2/c^2)^{-1/2}$ is the Lorentz factor, $v = (v_{\parallel}^2 + v_{\perp}^2)^{1/2}$ is the electron velocity, and v_{\parallel} and v_{\perp} are the electron velocity components parallel and perpendicular to the background magnetic field, respectively.

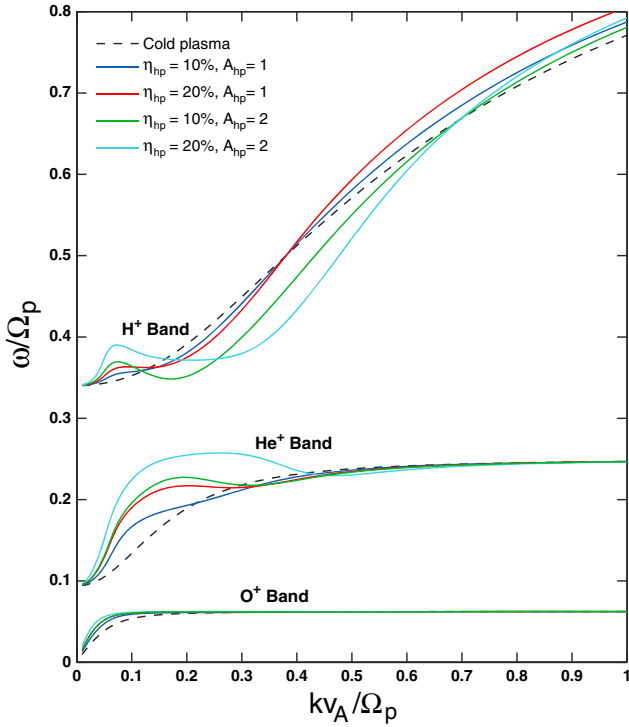


Figure 1. EMIC wave dispersion curves for H^+ , He^+ , and O^+ bands at $L = 4.5$. The dashed curves correspond to the cold plasma approximation, and the solid curves correspond to the hot plasma approaches for the four indicated sets of values for hot proton abundance η_{hp} and hot proton temperature anisotropy A_{hp} .

Since the resonance condition is independent on the perpendicular velocity v_{\perp} , we can readily obtain the electron minimum resonant energy E_{\min} by setting $v_{\perp} = 0$ (Silin et al., 2011),

$$E_{\min} \approx m_e c^2 \left(\sqrt{\frac{\Omega_e^2}{k^2 c^2} + 1} - 1 \right). \quad (4)$$

Equation (4) is derived from equation (6) of Summers and Thorne (2003) by using the approximation $\omega \ll |\Omega_e|$. It follows that E_{\min} is strictly dependent on the wave number k and that E_{\min} decreases with increasing k value.

The quasi-linear bounce-averaged pitch angle diffusion coefficient ($\langle D_{\alpha\alpha} \rangle$) can be expressed as (Summers et al., 2007b)

$$\langle D_{\alpha\alpha} \rangle = \frac{1}{\tau_B} \int_0^{\tau_B} D_{\alpha\alpha}(\alpha) \left(\frac{\partial \alpha_{\text{eq}}}{\partial \alpha} \right)^2 dt, \quad (5)$$

where τ_B is the particle bounce period, α and α_{eq} are the particle local and equatorial pitch angle, and the local pitch angle diffusion coefficient $D_{\alpha\alpha}$ is given by (Summers, 2005)

$$D_{\alpha\alpha} = D_{\mu\mu} / \sin^2 \alpha, \quad (6)$$

$$D_{\mu\mu} = \frac{\pi \Omega_e^2 (1 - \mu^2)}{2 W_0 \gamma^2} \sum_{j=1}^N \left(1 - \frac{\omega_j \mu}{k_j v} \right)^2 \frac{W(k_j)}{|v \mu - d\omega_j / dk_j|}, \quad (7)$$

where $\mu = \cos \alpha$, $W_0 = B_0^2 / 8\pi$ is the magnetic energy density of the background field, and $W(k_j)$ is the wave spectral density. The summation in equation (7) is carried out over the resonant roots of the wave frequency ω_j and wave number k_j (where $j = 1, 2, \dots, N$). For gyroresonant interactions between EMIC waves and electrons, ω_j and k_j are given by

the simultaneous solutions of the Doppler-shifted gyroresonance condition (equation (3)) and the EMIC wave dispersion relation (equation (1) or (2)). In the present study, we assume that EMIC wave spectral density has a Gaussian frequency distribution (Summers et al., 2007b),

$$\tilde{W}(\omega) = \frac{|\Delta B|^2}{8\pi} \frac{1}{\rho} \frac{1}{\delta\omega} e^{-\left(\frac{\omega - \omega_m}{\delta\omega}\right)^2}, \quad (8)$$

where ΔB is the mean wave amplitude, $\rho = \frac{\sqrt{\pi}}{2} \left[\text{erf} \left(\frac{\omega_m - \omega_{lc}}{\delta\omega} \right) + \text{erf} \left(\frac{\omega_{uc} - \omega_m}{\delta\omega} \right) \right]$, and ω_m and $\delta\omega$ are the frequency of maximum wave power and bandwidth, respectively; ω_{lc} and ω_{uc} are the lower and upper cutoffs of the wave spectrum, and erf is the error function. Following the study of Summers (2005), $W(k)$ in equation (7) can be expressed as

$$W(k) = \tilde{W}(\omega) \left| \frac{d\omega}{dk} \right| = \frac{|\Delta B|^2}{8\pi} \frac{1}{\rho} \frac{1}{\delta\omega} \left| \frac{d\omega}{dk} \right| e^{-\left(\frac{\omega - \omega_m}{\delta\omega}\right)^2}. \quad (9)$$

3. Numerical Results

We start by performing calculations for a particular set of realistic parameters. We focus on $L = 4.5$, representative of the heart of the Earth's outer radiation belt. The background magnetic field is assumed to be dipolar, and the electron density is adopted from the plasmaspheric density model of Sheeley et al. (2001). Following previous studies (e.g., He et al., 2016; Meredith et al., 2003; Summers et al., 2007a), we choose a typical set of ion composition ratios, that is, $\eta_p = 85\%$, $\eta_{He^+} = 10\%$, and $\eta_{O^+} = 5\%$. In this study, in addition to four cold particle species (cold e^- , p , He^+ , and O^+), hot anisotropic ring current protons are also included to investigate the kinetic effects of hot plasma on EMIC wave-driven scattering of radiation belt electrons. In Figure 1, we choose a fixed parallel temperature $T_{\parallel} = 25$ keV of hot protons and investigate the sensitivity of EMIC wave dispersion curves to the variation of hot proton abundance η_{hp} and temperature anisotropy A_{hp} . The wave

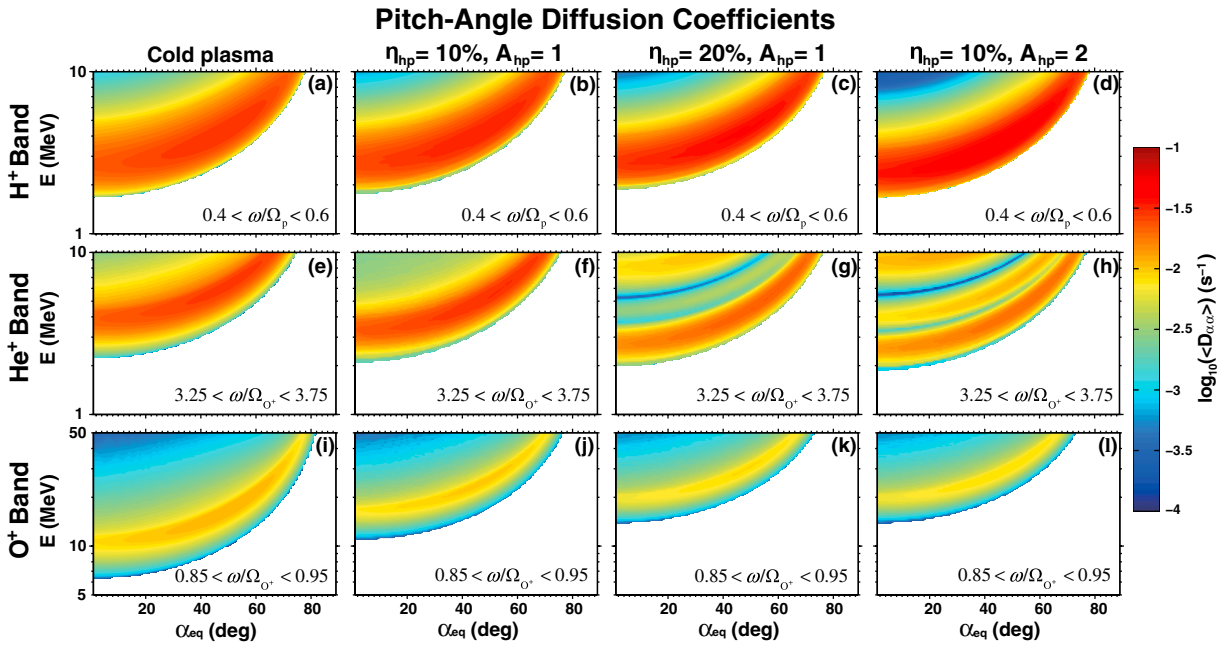


Figure 2. 2-D plots of bounce-averaged pitch angle diffusion coefficients $\langle D_{\alpha\alpha} \rangle$ as a function of electron kinetic energy E and equatorial pitch angle α_{eq} for (from top to bottom) all three emission bands at $L = 4.5$, for (from left to right) the cases of the cold plasma approximation and of the hot plasma approach including 10% hot protons with $A_{\text{hp}} = 1$, 20% hot protons with $A_{\text{hp}} = 1$, and 10% hot protons with $A_{\text{hp}} = 2$.

frequencies ω are normalized to the proton gyrofrequency Ω_p , and the wave numbers k are normalized to Ω_p/v_A , where v_A is the Alfvén velocity. The cold and hot plasma dispersion curves of EMIC waves are shown as the dashed and solid curves, respectively. It is clearly illustrated that inclusion of hot protons can lead to modification of the EMIC wave dispersion curves. A significant discrepancy between the cold and hot plasma dispersion curves only occurs at relatively small wave numbers for both He⁺ and O⁺ bands, while the discrepancy for H⁺ band dispersion curves can be found for almost all wave numbers. For the considered four pairs of η_{hp} (i.e., 10% or 20%) and A_{hp} (i.e., 1 or 2), the results show that for a fixed value of A_{hp} (η_{hp}) of hot protons, an increase of η_{hp} (A_{hp}) tends to result in a stronger modification of the EMIC wave dispersion curves.

On basis of computations of cold and hot plasma dispersion relations, as shown in Figure 1, we display in Figure 2 the 2-D plots of bounce-averaged pitch angle diffusion coefficients $\langle D_{\alpha\alpha} \rangle$ as a function of electron kinetic energy E and equatorial pitch angle α_{eq} for the three EMIC emission bands (H⁺, He⁺, and O⁺). We use a typical Gaussian wave spectrum with an amplitude of 1 nT for each band following previous studies (e.g., Albert, 2003; Summers & Thorne, 2003; Zhang et al., 2016). For H⁺ band waves, $\omega_{\text{lc}} = 0.4\Omega_p$, $\omega_{\text{uc}} = 0.6\Omega_p$, $\omega_m = 0.5\Omega_p$, and $\delta\omega = 0.1\Omega_p$; for He⁺ band waves, $\omega_{\text{lc}} = 3.25\Omega_{O^+}$, $\omega_{\text{uc}} = 3.75\Omega_{O^+}$, $\omega_m = 3.50\Omega_{O^+}$, and $\delta\omega = 0.25\Omega_{O^+}$; for O⁺ band waves, $\omega_{\text{lc}} = 0.85\Omega_{O^+}$, $\omega_{\text{uc}} = 0.95\Omega_{O^+}$, $\omega_m = 0.90\Omega_{O^+}$, and $\delta\omega = 0.05\Omega_{O^+}$. From the left to right, we show the results for the cold plasma approximation and the hot plasma approach including 10% hot protons with $A_{\text{hp}} = 1$, 20% hot protons with $A_{\text{hp}} = 1$, and 10% hot protons with $A_{\text{hp}} = 2$. Figure 2 shows that, in the cold plasma approximation, H⁺ and He⁺ band EMIC waves can pitch angle scatter multi-MeV electrons at a rate on the order of $>10^{-2.5} \text{ s}^{-1}$, indicating that these electrons are diffused into the loss cone in a time scale less than a few minutes. However, the results of diffusion coefficients in the hot plasmas can be modified by the kinetic effects introduced by hot anisotropic protons. It is shown that inclusion of 10% hot protons with $A_{\text{hp}} = 1$ can decrease the pitch angle diffusion rates of >5 MeV electrons at lower α_{eq} for H⁺ and He⁺ band EMIC waves. As η_{hp} increases to 20% or A_{hp} increases to 2, the pitch angle diffusion rates of >5 MeV electrons due to H⁺ band waves tend to decrease more significantly. For the pitch angle diffusion of >7 MeV electrons induced by He⁺ band waves, the increase of η_{hp} or A_{hp} can enhance the rates of scattering at $\alpha_{\text{eq}} < \sim 40^\circ$ and weaken the scattering efficiency at higher α_{eq} . Meanwhile, the increase of η_{hp} or A_{hp} tends to strongly reduce the pitch angle diffusion rates of <7 MeV electrons for He⁺ band waves.

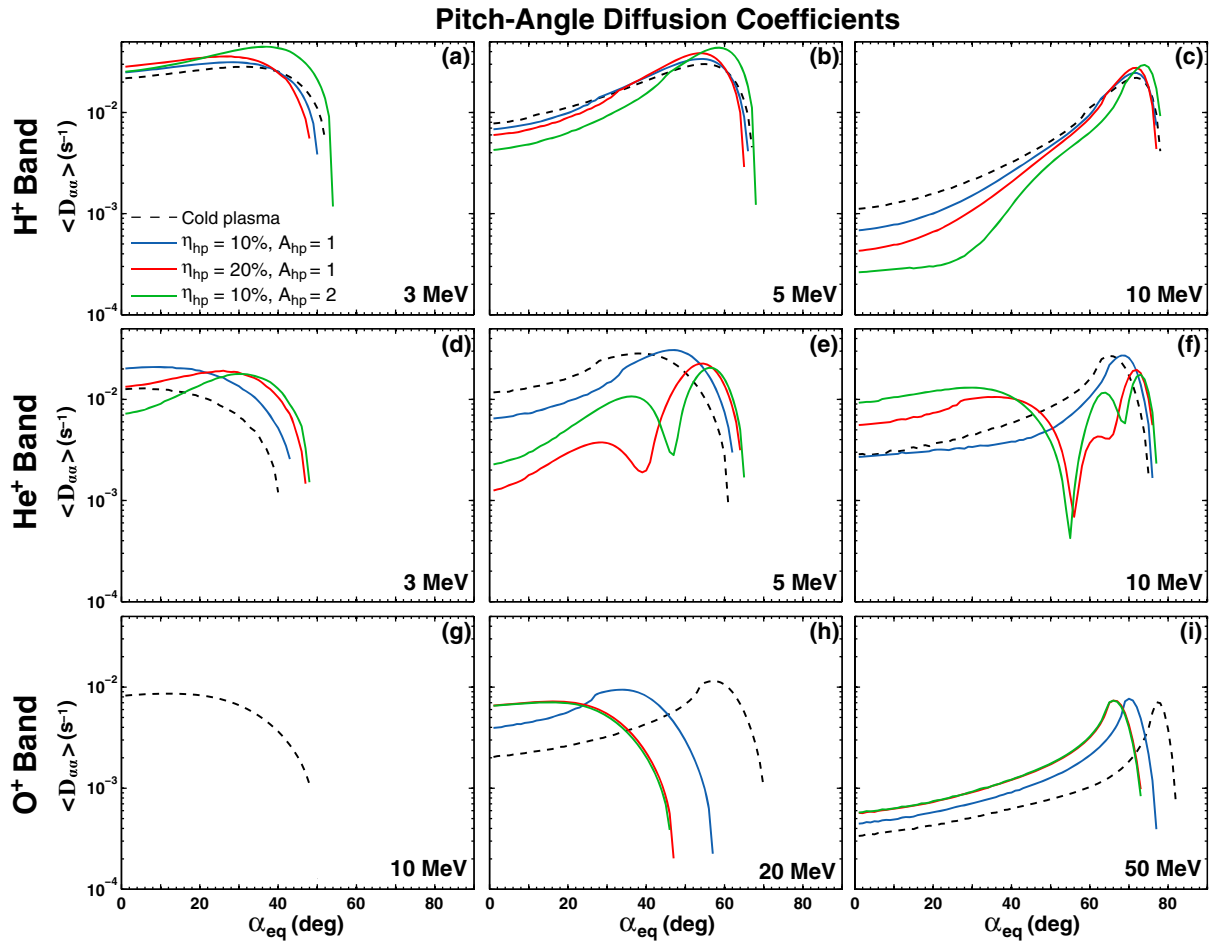


Figure 3. Line plots of bounce-averaged pitch angle diffusion coefficients $\langle D_{aa} \rangle$ as a function of equatorial pitch angle α_{eq} at $L = 4.5$, for the indicated electron energies corresponding to the three EMIC wave bands. The dashed black curve corresponds to the diffusion coefficients calculated from the cold plasma approximation, and the solid curves correspond to the diffusion coefficients calculated from the hot plasma approach for the three indicated sets of values for hot proton abundance and temperature anisotropy.

In addition, there are two pronounced minima of He^+ band-induced electron diffusion coefficients in the hot plasmas when $\eta_{hp} = 20\%$ or $A_{hp} = 2$. The corresponding electron energies at which the diffusion coefficients reach a minimum increase with α_{eq} result in two clear gaps in the 2-D plots of the pitch angle diffusion coefficients. While the electron minimum resonant energies due to H^+ and He^+ bands are not obviously affected by the hot plasma effects, the minimum resonant energies due to the O^+ band increase significantly with η_{hp} and A_{hp} . Therefore, O^+ band EMIC waves are unable to resonate with <10 MeV electrons in the hot plasmas when $\eta_{hp} \geq 10\%$ or $A_{hp} \geq 1$ since the minimum resonant energy exceeds 10 MeV. Overall, the pitch angle diffusion rates of highly relativistic electrons by O^+ band EMIC waves exhibit a general decreasing trend with η_{hp} and A_{hp} .

In Figure 3 we show the line plots of bounce-averaged electron pitch angle diffusion coefficients $\langle D_{aa} \rangle$ as a function of equatorial pitch angle α_{eq} at three indicated electron energies corresponding to H^+ , He^+ , and O^+ band EMIC waves. The black dashed curves correspond to diffusion coefficients calculated from the cold plasma approximation, and the solid curves correspond to those calculated from the hot plasma approach, for the three indicated sets of values of hot proton abundance and temperature anisotropy. Figure 3 illustrates that the diffusion coefficients of 3 and 5 MeV electrons due to the H^+ band is not significantly influenced by inclusion of the hot protons, while the scattering efficiency of 10 MeV electrons undergoes a pronounced decrease, especially at $\alpha_{eq} < 40^\circ$. For interactions between 3 MeV electrons and He^+ band waves, the pitch angle scattering at $\alpha_{eq} > \sim 20^\circ$ in the kinetic approach is found to be more efficient than that in the

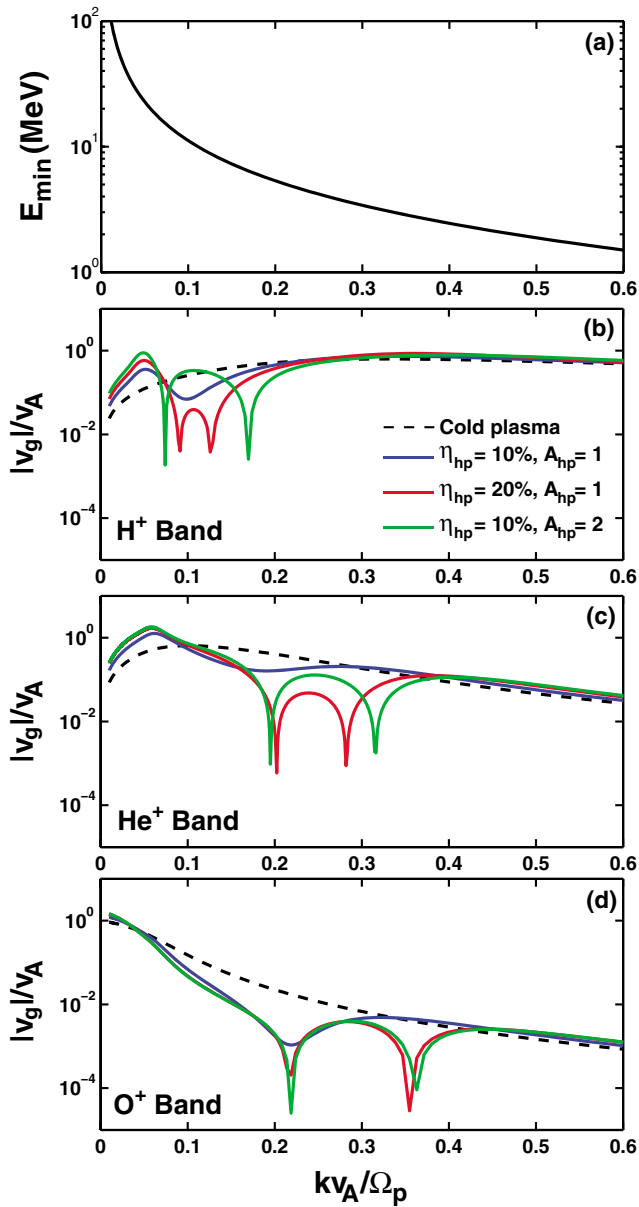


Figure 4. (a) Electron minimum resonant energy E_{\min} at the geomagnetic equator for $L = 4.5$, calculated based on equation (4), and normalized group velocities of (b) H^+ , (c) He^+ , and (d) O^+ bands as a function of normalized wave number. The black dashed curves indicate the group velocities for the cold plasma approximation and the solid curves for the three indicated sets of values for hot proton abundance and temperature anisotropy.

results clearly demonstrate that the hot plasma effects can strongly modify the EMIC wave group velocity, and this modification becomes more pronounced with the increase of η_{hp} or A_{hp} . For H^+ band EMIC waves, the significant modification of the group velocity is found at normalized $k < 0.2$, which corresponds to $E_{\min} > 5$ MeV. The group velocity values for 5–10 MeV electrons in the hot plasma approach are found to be smaller than those in the cold plasma approximation, which can help explain the weaker scattering efficiency of >5 MeV electrons indicated in Figure 2. For He^+ and O^+ band EMIC waves, the most significant discrepancy in the group velocity occurs at normalized $k > 0.1$, which corresponds to $E_{\min} < 10$ MeV. Since the associated electron minimum resonant energy for O^+ band in the hot plasma approach is higher than 10 MeV (as shown in Figure 2), the modification of the O^+ band group velocity does not significantly influence the

cold plasma approximation. Hot plasma effects can cause a significant decrease of the pitch angle diffusion coefficients of 5 MeV electrons at $\alpha_{eq} < 50^\circ$, thereby resulting in a large difference of up to an order of magnitude in diffusion coefficients between the cold and hot plasma approaches. This indicates that the scattering loss of 5 MeV electrons by He^+ band waves is seriously overestimated by the cold plasma approximation. For 10 MeV electrons, as η_{hp} increases to 20% or A_{hp} increases to 2, the diffusion coefficients at low α_{eq} increase to speed up the He^+ band wave-induced electron scattering loss, while the diffusion coefficients at $\alpha_{eq} \sim 50^\circ$ to 70° become much smaller. Thus, further work is required to understand how the loss time scale and the pitch angle distribution of these electrons are affected by the hot plasma effects. Figure 3 also illustrates that once contributions from the hot protons are taken into account, O^+ band EMIC waves cannot resonate with 10 MeV electrons. As well, the resonant coverage of α_{eq} for the cyclotron interactions between O^+ band waves and ultra-relativistic electrons narrows.

In order to examine the discrepancy in the diffusion coefficients between the cold and hot plasma approaches, we determine the electron minimum resonant energy E_{\min} (from equation (4)) and the normalized wave group velocity as functions of normalized wave number k at the geomagnetic equator for $L = 4.5$. The results are shown in Figure 4. Figure 4a indicates that E_{\min} decreases significantly with increasing values of k and can be less than 2 MeV for a relatively large k . It should be noted that for a fixed k , the corresponding wave frequency ω changes when hot protons are present (Figure 1). Therefore, for electrons with a fixed energy, inclusion of hot protons can change the resonant frequency and subsequently modify the corresponding wave spectral density given by equation (9). Since the local diffusion coefficient is proportional to the wave spectral density (equation (7)), the change of resonant wave frequency in hot plasmas can consequently influence the electron pitch angle scattering efficiency of EMIC waves.

From equation (9), we can see that the wave spectral density is proportional to the absolute value of wave group velocity $|v_g| = \left| \frac{d\omega}{dk} \right|$, which suggests that modification of EMIC wave group velocity by the hot plasma effects can also contribute to the discrepancy between the diffusion coefficients in the cold and hot plasma approaches. In Figures 4b–4d, we show the normalized group velocity of the EMIC waves as a function of normalized k for all three emission bands. The black dashed curve corresponds to the normalized group velocity calculated from the cold plasma approximation, and the solid curves correspond to the normalized values calculated from the hot plasma approach for the three indicated sets of values for η_{hp} and A_{hp} . The

magnitude of the electron pitch angle scattering rates due to the O^+ band. However, the modification of the He^+ band wave group velocity contributes significantly to the variations of electron pitch angle scattering rates. Figure 4c shows the discrepancy in the He^+ band group velocity curves for $E_{\min} = 3\text{--}10$ MeV. When $\eta_{hp} = 20\%$ or $A_{hp} = 2$, the discrepancies in group velocity become very pronounced and can be larger than 2 orders of magnitude at two specific values of wave number, and two local minima of the group velocity can be found. From equations (7) and (9), we see that the changes in group velocity introduced by the hot plasma effects can result in changes in diffusion coefficients to produce two minima at two specific values of E_{\min} where the group velocity itself reaches a minimum. Since E_{\min} is obtained by setting the perpendicular component of electron velocity $v_{\perp} = 0$, E_{\min} equals the electron kinetic energy E when $\alpha_{eq} = 0^\circ$. Therefore, for a fixed E_{\min} , E increases with increasing α_{eq} . It is expected that electron kinetic energies E at which the diffusion coefficients reach the minimum values increase with increasing α_{eq} . This is consistent with the results of the He^+ band wave-driven electron pitch angle scattering rates shown in Figure 2.

4. Discussions and Conclusions

This study aims to investigate the underlying role of hot plasma effects in the cyclotron-resonant interactions between multiband EMIC waves and radiation belt relativistic electrons by quantifying the bounce-averaged pitch angle diffusion coefficients using both the cold and hot plasma dispersion relations. Since the influence of hot plasma effects on the pitch angle scattering of electrons has a strong energy and pitch angle dependence, future modeling efforts are required to better understand the pitch angle evolution and scattering loss of ultra-relativistic electrons. Inclusion of hot plasma effects causes stronger scattering due to increased rates at some pitch angles and weaker scattering due to decreased rates at other pitch angles. However, these may not simply compensate each other. Scattering rates at higher pitch angles mainly determine the time scale that EMIC waves need to transport high pitch angle electrons to low pitch angles before the electron population reaches the equilibrium state (e.g., Ni et al., 2013). After the equilibrium state is reached, electrons at different pitch angles start to decay exponentially as a whole, and the associated loss time scale of the total electron population is then mainly controlled by the scattering rate near the edge of the loss cone (e.g., Summers et al., 2007b). In addition, if EMIC wave scattering is confined to small pitch angles and scattering at higher pitch angles is several orders of magnitude weaker, the loss of high pitch angle electrons may be controlled by this slow scattering to create a “bottle neck” in scattering (Albert & Shprits, 2009; Shprits et al., 2006).

Since the EMIC wave dispersion relation also plays an important role in EMIC wave-induced cyclotron-resonant scattering of ring current protons (Summers, 2005; Xiao et al., 2011) and bounce-resonant scattering of radiation belt electrons (Cao et al., 2017), it will also be of future interest to investigate the hot plasma effects on these scattering processes. Under geomagnetically active conditions, it is expected that modification of the resonant interactions between EMIC waves and magnetospheric particles by the hot plasma effects will be more pronounced due to enhanced activities of substorm injections. It is worthwhile to point out that, currently, there is certain uncertainty in the models of EMIC waves, including that the exact global distribution of the waves is difficult to obtain. This uncertainty may be comparable to or even larger than the hot plasma effects. When EMIC waves become very intense, it is likely for ultra-relativistic electrons to reach the strong diffusion (Schulz, 1974), which is limited by the size of the loss cone. Under such conditions, the electron loss rates may turn out to be independent on whether the hot plasma effects are taken into account or not.

It is worth noting that the present study focuses on the effects caused by variations in proton abundance and temperature anisotropy. In fact, a change in proton parallel temperature can also alter the wave dispersion relation so as to affect electron scattering by EMIC waves. Wang et al. (2016) showed that the hot plasma EMIC wave dispersion relation is more sensitive to the variation of proton abundance and temperature anisotropy, compared to the proton parallel temperature. Therefore, here we have selected a typical value of the ring current proton parallel temperature (i.e., 25 keV) to investigate the sensitivity of the EMIC wave dispersion relation to the other parameters. Although only the hot ring current protons are taken into consideration in this investigation, previous studies (Chen et al., 2011; Henning & Mace, 2014; Lee et al., 2017; Silin et al., 2011) have proved the importance of kinetic effects introduced by warm or hot heavier ions (He^+ and O^+) to the dispersive properties of EMIC waves. The modification of EMIC wave dispersion curves by warm or

hot heavier ions could be as important as that by hot protons. Therefore, once warm or hot heavier ions are present, their contributions also need to be included in future quantifications of electron minimum resonant energy and resultant diffusion coefficients in order to improve current understanding of electron scattering losses caused by EMIC waves. This, however, will be left as a future study.

The major conclusions of this study are summarized as follows:

1. Inclusion of hot protons can significantly affect EMIC wave-induced pitch angle scattering of radiation belt electrons by modifying the dispersion relation for each of the three (H^+ , He^+ , and O^+) wave bands. The hot plasma modification of electron pitch angle scattering rates becomes more pronounced with the increase of hot proton abundance or temperature anisotropy.
2. For H^+ band EMIC waves, hot plasma effects tend to weaken the pitch angle scattering efficiency of >5 MeV electrons. He^+ band EMIC wave-induced scattering of >3 MeV electrons is most sensitive to the hot plasma effects, showing a large difference up to an order of magnitude in the diffusion coefficients between the cold and hot plasma approaches. While hot plasma effects do not greatly change the minimum resonant energies for H^+ and He^+ band EMIC waves, they can cause a strong increase of the electron minimum resonant energy for O^+ band waves, thereby making it difficult for O^+ band EMIC waves to resonate effectively with <10 MeV electrons.
3. Significant discrepancies between the cold and hot plasma approaches are found in the electron minimum resonant energy and pitch angle diffusion coefficients for multiband EMIC waves. The discrepancies are mainly caused by changes in resonant frequency and wave group velocity introduced by the inclusion of hot anisotropic protons.

Our study confirms the importance of including hot plasma effects in calculations of radiation belt electron scattering rates by EMIC waves when the hot plasma dispersion relation deviates significantly from the cold plasma approximation. Clearly, hot plasma effects need to be carefully incorporated into future simulations of radiation belt electron dynamics, especially during geomagnetically disturbed periods. At the same time, we note that during such periods, pitch angle scattering may approach strong diffusion whether or not hot plasma effects are taken into account.

Acknowledgments

The work was supported by the NSFC grants 41674163, 41474141, and 41204120 and the Hubei Province Natural Science Excellent Youth Foundation (2016CFA044). D.S. acknowledges support from a discovery grant of the Natural Sciences and Engineering Research Council of Canada. Y.Y.S. acknowledges support from EU Horizon 2020 637302 and DFG SFB 1294. No data sets are used for this study.

References

- Albert, J. M. (2003). Evaluation of quasi-linear diffusion coefficients for EMIC waves in a multispecies plasma. *Journal of Geophysical Research*, 108(A6), 1249. <https://doi.org/10.1029/2002JA009792>
- Albert, J. M., & Shprits, Y. Y. (2009). Estimates of lifetimes against pitch angle diffusion. *Journal of Atmospheric and Solar - Terrestrial Physics*, 71(16), 1647–1652. <https://doi.org/10.1016/j.jastp.2008.07.004>
- Anderson, B. J., Denton, R. E., Ho, G., Hamilton, D. C., Fuselier, S. A., & Strangeway, R. J. (1996). Observational test of local proton cyclotron instability in the Earth's magnetosphere. *Journal of Geophysical Research*, 101(A10), 21,527–21,543. <https://doi.org/10.1029/96JA01251>
- Cao, X., Ni, B., Liang, J., Xiang, Z., Wang, Q., Shi, R., ... Liu, J. (2016). Resonant scattering of central plasma sheet protons by multiband EMIC waves and resultant proton loss timescales. *Journal of Geophysical Research: Space Physics*, 121, 1219–1232. <https://doi.org/10.1002/2015JA021933>
- Cao, X., Ni, B., Summers, D., Bortnik, J., Tao, X., Shprits, Y. Y., ... Wang, Q. (2017). Bounce resonance scattering of radiation belt electrons by H^+ band EMIC waves. *Journal of Geophysical Research: Space Physics*, 122, 1702–1713. <https://doi.org/10.1002/2016JA023607>
- Chen, L., Thorne, R. M., & Bortnik, J. (2011). The controlling effect of ion temperature on EMIC wave excitation and scattering. *Geophysical Research Letters*, 38, L16109. <https://doi.org/10.1029/2011GL048653>
- Chen, L., Thorne, R. M., Shprits, Y., & Ni, B. (2013). An improved dispersion relation for parallel propagating electromagnetic waves in warm plasmas: Application to electron scattering. *Journal of Geophysical Research: Space Physics*, 118, 2185–2195. <https://doi.org/10.1002/jgra.50260>
- Fried, B. D., & Conte, S. D. (1961). *The plasma dispersion function*. New York: Academic Press.
- Gary, S. P. (1993). *Theory of space plasma microinstabilities* (pp. 126–127). New York: Cambridge University Press. <https://doi.org/10.1017/CBO9780511551512>
- Gary, S. P., Moldwin, M. B., Thomsen, M. F., Winske, D., & McComas, D. J. (1994). Hot proton anisotropies and cool proton temperatures in the outer magnetosphere. *Journal of Geophysical Research*, 99(A12), 23,603–23,615. <https://doi.org/10.1029/94JA02069>
- He, F., Cao, X., Ni, B., Xiang, Z., Zhou, C., Gu, X., ... Wang, Q. (2016). Combined scattering loss of radiation belt relativistic electrons by simultaneous three-band EMIC waves: A case study. *Journal of Geophysical Research: Space Physics*, 121, 4446–4451. <https://doi.org/10.1002/2016JA022483>
- Henning, F. D., & Mace, R. L. (2014). Effects of ion abundances on electromagnetic ion cyclotron wave growth rate in the vicinity of the plasmapause. *Physics of Plasmas*, 20, 042905. <https://doi.org/10.1063/1.4873375>
- Horne, R. B., & Thorne, R. M. (1997). Wave heating of He^+ by electromagnetic ion cyclotron waves in the magnetosphere: Heating near the $H^+ - He^+$ bi-ion resonance frequency. *Journal of Geophysical Research*, 102(A6), 11,457–11,471. <https://doi.org/10.1029/97JA00749>
- Jordanova, V. K., Farrugia, C. J., Thorne, R. M., Khazanov, G. V., Reeves, G. D., & Thomsen, M. F. (2001). Modeling ring current proton precipitation by electromagnetic ion cyclotron waves during the May 14–16, 1997, storm. *Journal of Geophysical Research*, 106(A1), 7–22. <https://doi.org/10.1029/2000JA002008>

- Kozyra, J., Cravens, T., Nagy, A., Fontheim, E., & Ong, R. (1984). Effects of energetic heavy ions on electromagnetic ion cyclotron wave generation in the plasmopause region. *Journal of Geophysical Research*, *89*(A4), 2217–2233. <https://doi.org/10.1029/JA089iA04p02217>
- Lee, J. H., Chen, L., Angelopoulos, V., & Thorne, R. M. (2012). THEMIS observations and modeling of multiple ion species and EMIC waves: Implications for a vanishing He⁺ stop band. *Journal of Geophysical Research*, *117*, A06204. <https://doi.org/10.1029/2012JA017539>
- Lee, D.-Y., Noh, S.-J., Choi, C.-R., Lee, J. J., & Hwang, J. A. (2017). Effect of hot anisotropic He⁺ ions on the growth and damping of electromagnetic ion cyclotron waves in the inner magnetosphere. *Journal of Geophysical Research: Space Physics*, *122*, 4935–4942. <https://doi.org/10.1002/2016JA023826>
- Liang, J., Donovan, E., Ni, B., Yue, C., Jiang, F., & Angelopoulos, V. (2014). On an energy-latitude dispersion pattern of ion precipitation potentially associated with magnetospheric EMIC waves. *Journal of Geophysical Research: Space Physics*, *119*, 8137–8160. <https://doi.org/10.1002/2014JA020226>
- Liu, K., Winske, D., Gary, S. P., & Reeves, G. D. (2012). Relativistic electron scattering by large amplitude electromagnetic ion cyclotron waves: The role of phase bunching and trapping. *Journal of Geophysical Research*, *117*, A06218. <https://doi.org/10.1029/2011JA017476>
- Meredith, N. P., Thorne, R. M., Horne, R. B., Summers, D., Fraser, B. J., & Anderson, R. R. (2003). Statistical analysis of relativistic electron energies for cyclotron resonance with EMIC waves observed on CRRES. *Journal of Geophysical Research*, *108*(A6), 1250. <https://doi.org/10.1029/2002JA009700>
- Meredith, N. P., Horne, R. B., Kersten, T., Fraser, B. J., & Grew, R. S. (2014). Global morphology and spectral properties of EMIC waves derived from CRRES observations. *Journal of Geophysical Research: Space Physics*, *119*, 5328–5342. <https://doi.org/10.1002/2014JA020064>
- Min, K., Liu, K., Bonnell, J. W., Breneman, A. W., Denton, R. E., Funsten, H. O., ... Wygant, J. R. (2015). Study of EMIC wave excitation using direct ion measurements. *Journal of Geophysical Research: Space Physics*, *120*, 2702–2719. <https://doi.org/10.1002/2014JA020717>
- Ni, B., Bortnik, J., Thorne, R. M., Ma, Q., & Chen, L. (2013). Resonant scattering and resultant pitch angle evolution of relativistic electrons by plasmaspheric hiss. *Journal of Geophysical Research: Space Physics*, *118*, 7740–7751. <https://doi.org/10.1002/2013JA019260>
- Ni, B., Cao, X., Zou, Z., Zhou, C., Gu, X., Bortnik, J., ... Xie, L. (2015). Resonant scattering of outer zone relativistic electrons by multiband EMIC waves and resultant electron loss time scales. *Journal of Geophysical Research: Space Physics*, *120*, 7357–7373. <https://doi.org/10.1002/2015JA021466>
- Saikin, A. A., Zhang, J.-C., Allen, R. C., Smith, C. W., Kistler, L. M., Spence, H. E., ... Jordanova, V. K. (2015). The occurrence and wave properties of H⁺, He⁺, and O⁺-band EMIC waves observed by the Van Allen Probes. *Journal of Geophysical Research: Space Physics*, *120*, 7477–7492. <https://doi.org/10.1002/2015JA021358>
- Schulz, M. (1974). Particle lifetimes in strong diffusion. *Astrophysics and Space Science*, *31*(1), 37–42. <https://doi.org/10.1007/BF00642599>
- Sheeley, B. W., Moldwin, M. B., Rassoul, H. K., & Anderson, R. R. (2001). An empirical plasmasphere and trough density model: CRRES observations. *Journal of Geophysical Research*, *106*(A11), 25,631–25,641. <https://doi.org/10.1029/2000JA000286>
- Shprits, Y. Y. (2009). Potential waves for pitch angle scattering of near-equatorially mirroring energetic electrons due to the violation of the second adiabatic invariant. *Geophysical Research Letters*, *36*, L12106. <https://doi.org/10.1029/2009GL038322>
- Shprits, Y. Y., Li, W., & Thorne, R. M. (2006). Controlling effect of the pitch angle scattering rates near the edge of the loss cone on electron lifetimes. *Journal of Geophysical Research*, *111*, A12206. <https://doi.org/10.1029/2006JA011758>
- Shprits, Y. Y., Subbotin, D. A., Meredith, N. P., & Elkington, S. R. (2008). Review of modeling of losses and sources of relativistic electrons in the outer radiation belts: II. Local acceleration and loss. *Journal of Atmospheric and Solar - Terrestrial Physics*, *70*(14), 1694–1713. <https://doi.org/10.1016/j.jastp.2008.06.014>
- Shprits, Y. Y., Subbotin, D., Drozdov, A., Usanova, M. E., Kellerman, A., Orlova, K., ... Kim, K. C. (2013). Unusual stable trapping of the ultrarelativistic electrons in the Van Allen radiation belts. *Nature Physics*, *9*(11), 699–703. <https://doi.org/10.1038/nphys2760>
- Shprits, Y. Y., Drozdov, A. Y., Spasojevic, M., Kellerman, A. C., Usanova, M. E., Engebretson, M. J., ... Aseev, N. A. (2016). Wave-induced loss of ultra-relativistic electrons in the Van Allen radiation belts. *Nature Communications*, *7*, 12,883. <https://doi.org/10.1038/ncomms12883>
- Shprits, Y. Y., Kellerman, A., Aseev, N., Drozdov, A. Y., & Michaelis, I. (2017). Multi-MeV electron loss in the heart of the radiation belts. *Geophysical Research Letters*, *44*, 1204–1209. <https://doi.org/10.1002/2016GL072258>
- Silin, I., Mann, I. R., Sydora, R. D., Summers, D., & Mace, R. L. (2011). Warm plasma effects on electromagnetic ion cyclotron wave MeV electron interactions in the magnetosphere. *Journal of Geophysical Research*, *116*, A05215. <https://doi.org/10.1029/2010JA016398>
- Stix, T. H. (1962). *The theory of plasma waves* (p. 34). New York: McGraw-Hill.
- Summers, D. (2005). Quasi-linear diffusion coefficients for field-aligned electromagnetic waves with applications to the magnetosphere. *Journal of Geophysical Research*, *110*, A08213. <https://doi.org/10.1029/2005JA011159>
- Summers, D., & Thorne, R. M. (2003). Relativistic electron pitch angle scattering by electromagnetic ion cyclotron waves during geomagnetic storms. *Journal of Geophysical Research*, *108*(A4), 1143. <https://doi.org/10.1029/2002JA009489>
- Summers, D., Ni, B., & Meredith, N. P. (2007a). Timescales for radiation belt electron acceleration and loss due to resonant wave-particle interactions: 2. Evaluation for VLF chorus, ELF hiss, and electromagnetic ion cyclotron waves. *Journal of Geophysical Research*, *112*, A04207. <https://doi.org/10.1029/2006JA011993>
- Summers, D., Ni, B., & Meredith, N. P. (2007b). Timescales for radiation belt electron acceleration and loss due to resonant wave-particle interactions: 1. Theory. *Journal of Geophysical Research*, *112*, A04206. <https://doi.org/10.1029/2006JA011801>
- Thorne, R. M., & Horne, R. B. (1997). Modulation of electromagnetic ion cyclotron instability due to interaction with ring current O⁺ during magnetic storms. *Journal of Geophysical Research*, *102*, 14,155–14,164.
- Thorne, R. M., & Kennel, C. F. (1971). Relativistic electron precipitation during magnetic storm main phase. *Journal of Geophysical Research*, *76*(19), 4446–4453. <https://doi.org/10.1029/JA076i019p04446>
- Usanova, M. E., Mann, I. R., Kale, Z. C., Rae, I. J., Sydora, R. D., Sandanger, M., ... Vallières, X. (2010). Conjugate ground and multisatellite observations of compression-related EMIC Pc1 waves and associated proton precipitation. *Journal of Geophysical Research*, *115*, A07208. <https://doi.org/10.1029/2009JA014935>
- Usanova, M. E., Drozdov, A., Orlova, K., Mann, I. R., Shprits, Y., Robertson, M. T., ... Wygant, J. (2014). Effect of EMIC waves on relativistic and ultrarelativistic electron populations: Ground-based and Van Allen Probes observations. *Geophysical Research Letters*, *41*, 1375–1381. <https://doi.org/10.1002/2013GL059024>
- Wang, Q., Cao, X., Gu, X., Ni, B., Zhou, C., Shi, R., & Zhao, Z. (2016). A parametric study of the linear growth of magnetospheric EMIC waves in a hot plasma. *Physics of Plasmas*, *23*(6), 062903. <https://doi.org/10.1063/1.4953565>

- Xiao, F., Chen, L., He, Y., Su, Z., & Zheng, H. (2011). Modeling of precipitation loss of ring current protons by electromagnetic ion cyclotron waves. *Journal of Atmospheric and Solar - Terrestrial Physics*, 73(1), 106–111. <https://doi.org/10.1016/j.jastp.2010.01.007>
- Zhang, J.-C., Kistler, L. M., Mouikis, C. G., Klecker, B., Sauvaud, J.-A., & Dumlop, M. W. (2011). A statistical study of EMIC wave-associated He⁺ energization in the outer magnetosphere: Cluster/CODIF observations. *Journal of Geophysical Research*, 116, A11201. <https://doi.org/10.1029/2011JA016690>
- Zhang, X.-J., Li, W., Thorne, R. M., Angelopoulos, V., Bortnik, J., Kletzing, C. A., ... Hospodarsky, G. B. (2016). Statistical distribution of EMIC wave spectra: Observations from Van Allen Probes. *Geophysical Research Letters*, 43, 12,348–12,355. <https://doi.org/10.1002/2016GL071158>